Journal of Power Sources 262 (2014) 140–146

Contents lists available at ScienceDirect

Journal of Power Sources

journal homepage: www.elsevier.com/locate/jpowsour

Enhanced photovoltaic properties of modified redox electrolyte in dye-sensitized solar cells using tributyl phosphate as additive

Malihe Afrooz, Hossein Dehghani*

Department of Inorganic Chemistry, Faculty of Chemistry, University of Kashan, P.O. Box 87317-51167, Kashan, Iran

HIGHLIGHTS

- TBPP suppresses the electron recombination that leads to the increase in J_{sc}.
- The TBPP additive also causes to accumulation of electrons in the CB of TiO_2.
- The TBPP additive shifts the CB that leads to significantly improvement in V_{oc}.
- This simple modification can significantly improve the performance of DSSCs.

ARTICLE INFO

Article history:
Received 18 December 2013
Received in revised form
9 March 2014
Accepted 24 March 2014
Available online 1 April 2014

Keywords:
Dye-sensitized solar cell
Tributyl phosphate
Additive
Electron recombination
2-Cyano-3-(4-(diphenylamino)phenyl)
acrylic acid
Electrolyte

ABSTRACT

In this study, we report the influence of a phosphate additive on the performance of dye-sensitized solar cells (DSSCs) based on 2-cyano-3-(4-(diphenylamino)phenyl)acrylic acid (TPA) as sensitizer. The DSSCs are fabricated by incorporating tributyl phosphate (TBPP) as an additive in the electrolyte and is attained an efficiency of about 3.03% under standard air mass 1.5 global (AM 1.5G) simulated sunlight, corresponding to 35% efficiency increment compare to the standard liquid electrolyte. An improvement in both open circuit voltage (V_{oc}) and short circuit current (J_{sc}) obtains by adjusting the concentration of TBPP in the electrolyte, which attributes to enlarge energy difference between the Fermi level (E_F) of TiO_2 and the redox potential of electrolyte and suppression of charge recombination from the conduction band (CB) of TiO_2 to the oxidized ions in the redox electrolyte. Electrochemical impedance analyses (EIS) reveals a dramatic increase in charge transfer resistance at the dyed-TiO_2/electrolyte interface and the electron density in the CB of TiO_2 that the more prominent photoelectric conversion efficiency (η) improvement with TBPP additive results by the efficient inhibition of recombination processes. This striking result leads to use a family of electron donor groups in many compounds as highly efficient additive.

1. Introduction

Dye-sensitized solar cells (DSSCs) have been extensively studied in many dissertations because of their simplicity, low cost manufacturing and relatively high energy conversion efficiency obtained at diffuse light intensities [1–3]. Since O'Regan and Gratzel's pioneering report in 1991 [4], the efficiency slowly progressed over the years toward above 14% in 2013 [5]. Nowadays, many studies are focused on the dyes and electrolytes that form the key components of a DSSC [6–11]. The relatively high cost of the ruthenium metal complexes and complicated synthesis process limit their large scale applications in DSSCs. For these reasons, metal-free organic dye sensitizers such as squaraine [12], indoline [13], carbazole [14], triarylamine [15,16], tetrahydroquinoline [17], coumarin [18], fluorine [19], phthalocyanins [20,21] and porphyrins [22–25] that can be less expensive, have been under rapid development and used in DSSCs as appropriate photosensitizer. The significant structural diversity of organic molecules allows to designing dyes with broad and strong absorption across the visible and near infrared regions and high absorption coefficients. But, a major problem for many organic dyes is dye aggregation on the semiconductor surface that reduces conversion efficiency in DSSCs. Among the organic dyes, triphenylamine and its derivatives have become promising candidates used as well-known compounds in DSSCs, because the triphenylamine molecule has a non-coplanar structure and can act as excellent electron donating [26–29]. However, triphenylamine sensitizers will require multistep synthesis, but, experimental and theoretical studies have demonstrated that the steric properties of triphenylamine unit may prevent

* Corresponding author. Tel.: +98 361 5912386; fax: +98 361 591 2397.
E-mail address: dehghani@kashanu.ac.ir (H. Dehghani).

http://dx.doi.org/10.1016/j.jpowsour.2014.03.115
0378-7753/

unfavorable dye aggregation on the TiO_2 surface. In addition to the modification of sensitizers, addition of the additives in liquid electrolytes is a convenient way to improve photovoltaic performance [30,31]. The adsorption of additives on the photoanode surface have been found to exert influences on many parameters and important processes in a cell, such as semiconductor surface charge, the conduction band edge, electron injection and electron recombination kinetics that due to formation of an insulating layer on electrode surface. This layer elevates the conduction band (CB) of semiconductor and represses electron recombination. For the first time, in 1993, 4-tert-butylpyridine (TBP) was employed as an additive in iodide/triiodide electrolyte and was observed a significant improvement of the open circuit voltage (V_{oc}) [32]. Increasing of the V_{oc} could be ascribed to a combined effect of the high electron density in the CB of TiO_2 and the slower electron recombination rate that leads to shift of Fermi level (E_F) in TiO_2. With this consideration, a great deal of efforts have been devoted to apply many compounds or cations as an additive for optimization or development the iodide/triiodide system such as *N*-alkylbenzimidazoles [33], pyridine analogs [34], lithium [35] and guanidinium [36] ions.

Recently, Dai et al. introduced an impressive phosphate additive for iodine electrolyte to modify the dyed-TiO_2/electrolyte interface and a major improvement in cell performance was obtained compared to the standard electrolyte [37]. The efficiency of 9.50% was obtained for optimum device by soaking in N719 for 12 h after applying tributyl phosphate (TBPP) as additive in the iodine electrolyte. This value is higher than the cell in which standard iodine electrolyte is used (6.74%). Interaction between additives and TiO_2 surface is not clear completely, so, it is very important to understand the effect of this interaction on the electron injection yield, electron diffusion coefficient and transport and recombination processes in improvement the performance of DSSCs. Herein, this finding encouraged us to apply this additive with 2-cyano-3-(4-(diphenylamino)phenyl)acrylic acid (TPA) dye and study their precise action on the cell parameters. First, we synthesized TPA and used it as sensitizer in our devices. Modified electrolyte consisting of the iodide/triiodide electrolyte with TBPP additive was applied in the cells. Furthermore, the influence of different concentrations of the additive on the cell performance was studied. When the concentration of TBPP in the electrolyte was increased to 1 M, a 35% energy conversion efficiency increment was exhibited. The results of this study can be help to develop a simple and effective method to improve V_{oc}, short circuit current (J_{sc}) and η in the DSSCs. Iodide/triiodide redox couple has studied as common electrolyte in most of DSSCs, so, modified electrolyte by new compounds prove low cost method for commercial that can be used in large scale.

2. Experimental

2.1. Materials and instrumentation

All chemical materials and solvents used for synthesis were purchased from Merck and Sigma–Aldrich Companies. For preparation of dry acetonitrile in the electrolytes it was kept over 4 Å molecular sieves for 24 h.

^{1}H NMR spectrum were recorded (DMSO-d_6) on Bruker DPX-400 MHz NMR spectrometer. UV–visible absorption spectrum of the dye solution was obtained with a GBC cintra 6 UV–visible spectrophotometer. The FT-IR spectrum was recorded by using a Magna 550 Nicolet spectrometer using KBr pellets.

2.2. Synthesis of TPA dye

(4-Diphenyl amino)benzaldehyde was synthesized according to the literature [15,38]. (4-Diphenyl amino)benzaldehyde (0.74 mmol, 205 mg) was dissolved in 15 mL of acetonirile in a three-necked flask. Cyano-acetic acid (1.49 mmol, 127 mg) and a few drops of piperidine (1.12 mmol, 95 mg) as catalyst was placed in flask and heated under reflux for 12 h at argon atmosphere and the reaction was followed by TLC. After completion of the reaction, the mixture was cooled down to room temperature and the solvent is removed by rotary evaporation. The residue was extracted with dichloromethane and 0.1 M HCl solution. Organic phase was purified by silicagel column chromatography with dichloromethane/methanol (6:1, v:v) as eluent to afford the dye TPA as a deep yellow solid, 146 mg (yield 71%), Scheme 1.

UV–vis (THF), λ_{max} (nm): 296, 416, 836; IR (KBr), ν (cm^{-1}): 3443 (ν_{O-H}, s), 2214 ($\nu_{C\equiv N}$, s), 1619 ($\nu_{C=O}$, s), 1585 ($\nu_{C=C}$, s), 1496 ($\nu_{C=C}$, s), 1184 (ν_{C-O}, s), 756 (s), 698 (s), 621 (s); ^{1}H NMR (DMSO-d_6), δ (ppm); 7.87 (1H, s, –CH=), 7.59 (2H, d, Ar–H), 7.39 (4H, t, Ar–H), 7.14 (6H, m, Ar–H), 6.88 (2H, d, Ar–H).

2.3. Fabrication of photovoltaic devices

To prepare transparent working electrodes, the fluorine doped tin oxide coated glass substrates (FTO) (Solaronix TEC Glass-TEC 8, solar 2.3 mm thickness) were first cleaned with deionized water, acetone and ethanol in an ultrasonic bath. A standard TiO_2 (P25, Degussa, Germany) paste was prepared following procedure. Briefly, 1 g of TiO_2 was mixed by 0.2 mL of acetic acid and grind in a mortar for 5 min. 2 mL of water and 10 mL of ethanol were added into the mixture and were dispersed with an ultrasonic horn for 15 min, followed by stirring for 30 min to form a slurry solution mixture. Then, 2 g of terpineol and 0.5 mL of ethyl cellulose solution (10 wt% solution in ethanol) were added into the TiO_2 suspension and followed by sonication for 15 min. The mixture was stirred and was concentrated by evaporation of the ethanol at room temperature to form a viscous TiO_2 paste. The FTO plates were soaked in 40 mM aqueous $TiCl_4$ solution at 70 °C for 30 min and washed with water and dried in air. For obtain a double-layer TiO_2 photoelectrode, the TiO_2 paste was deposited onto the FTO plates by doctor blade method and then was dried at 120 °C for 5 min. The coated bilayer films were gradually heated to 500 °C and were calcined for 15 min. Subsequently, for surface modification, the electrodes were immersed into the $TiCl_4$ aqueous as described previously and then were calcined at 500 °C for 15 min. After cooling to 80 °C, the film was put into the dye solution (0.3 mM of dye in THF) and maintained for 2 h at room temperature. For preparing of counter electrodes, a thin layer of Pt was deposited onto the FTO glass by thermal decomposition of

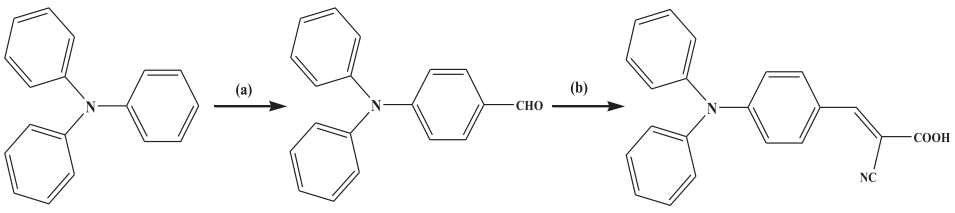

Scheme 1. (a) $POCl_3$, DMF, 1,2-dichloroethane, reflux, 8 h [15,38] (b) 2-cyanoacetic acid, piperidine, acetonitrile, reflux, 12 h.

a drop of H_2PtCl_6 solution (2 mg of Pt in 1 mL of ethanol). The working and counter electrodes were assembled into a sandwich configuration using a 30 μm surlyn spacer (Dyesol, Australia). The modified electrolytes containing 0.1 M LiI, 0.05 M I_2, 0.5 M TBP, 0.6 M 1-butyl-2,3-dimethylimidazolium iodide (BDMII) and different concentrations of TBPP in dry acetonitrile, were placed on the hole in the counter electrode via capillary action. Finally, the devices were sealed by a piece of surlyn film and a coverslip (0.1 mm thickness).

2.4. Photovoltaic and electrical impedance measurement

Cyclic voltammetry (CV) was used to study the electrochemical properties of the electrolytes. The CV spectra were obtained with a Sama 500 potentiostat (Isfahan, Iran) using 0.1 M lithium perchlorate trihydrate in acetonitrile as a supporting electrolyte. An Ag/AgCl/KCl(sat.) as a reference electrode, a glassy carbon working electrode (2 mm diameter) and platinum wire counter electrode were employed. The thickness of the transparent mesoporous TiO_2 layer was determined using surface profilometer. The electrochemical impedance spectroscopy (EIS) measurements of the cells were achieved under AM 1.5 G simulated light (Luzchem) using potantiostat/galvanostat (PGSTAT 100, Autolab, Eco-Chemie), at an AC amplitude of 5 mV within the frequency range from 0.01 Hz to 100 kHz in the dark. The photocurrent–voltage (I–V) characteristics of the cells were measured using a Keithley model 2400 digital source meter (Keithley, USA). The obtained spectra from the EIS measurements were fitted by Z-view software (v2.9c, Scribner Associates Inc.). In our study, we repeated the processes of the prepared cells for several times until avoid errors in the results.

3. Results and discussion

3.1. Spectral and electrochemical properties of dye

In many investigations the analytical and spectroscopic data were proved that the cyanoacrylic acid anchoring group in the photosensitizer have a strongly bind onto the semiconductor surface. Also, the dyes with this group have suitable excited and ground state energy levels to matching with electrolyte potential and the E_F of the semiconductor [39,40]. On the other hand, the self-association or aggregation of dye molecules in solution or on the semiconductor surface decreases J_{sc} in the DSSC. If the aggregation of dye be substantial on the TiO_2 surface, a shift may be observed in spectral band position in the absorption, reflectance, transmittance or emission spectrum of a molecule to a longer or shorter wavelength. The desirable electronic and steric properties of triphenylamine dyes caused to prevent dye aggregation on the anode surface. The UV–vis absorption of TPA dye in solution and on anode films with use no additive in the dye solution displayed a little red shift on the surface which can be ascribed to the formation of a little J-type aggregate and interaction of the anchoring group with the TiO_2 surface that has negligible effect on the cell performance [41]. According to the UV–vis spectra, this dye exhibits two major broad bands, appearing at ca. 416 nm and ca. 296 nm. The strong absorption band around 416 nm can be corresponded to HOMO to LUMO transitions (an intramolecular charge transfer (ICT) between the triphenylamine donor and the acceptor end group), while the absorption band in the UV region in the 296 nm was assigned to a π–π^* transition.

To investigate the process of electron transfer at the device, the HOMO and LUMO energy levels of the dye were estimated by using CV [41]. To complete the electron injection into the CB of TiO_2 from the excited dye molecule, the value of $E_{ox} - E_{0-0}$ must be sufficiently negative than E_{CB} in the TiO_2. The LUMO level of the TPA dye was measured by $E_{ox} - E_{0-0}$, in which E_{0-0} was determined by the absorption thresholds from spectrum of dye adsorbed on the TiO_2 film. The ground state oxidation potential of TPA (corresponding to the HOMO level) is 1.33 V vs. NHE. Electrochemical data for the TPA dye that has been obtained from reference 41are summarized in Table 1.

Table 1
Absorption, emission, and electrochemical properties of TPA dye [41].

Dye	λ_{max} (abs)[a] [nm]	λ_{max} (em)[a] [nm]	E_{ox}[b] [V vs. NHE]	λ_{max} on TiO_2 [nm]	E_{0-0} abs/em [V]	$E_{ox} - E_{0-0}$ [V vs. NHE]
TPA	381	515	1.33	405	2.63	−1.30

[a] Absorption and emission spectra of dye in CH_3CN (2×10^{-5} M) at room temperature.
[b] The oxidation potential of the dye was measured in condition that was described in Section 2.4.

Table 2
Solar cell performance parameters obtained using the phosphate additive under AM 1.5 (100 mW cm^{-2}) illumination with an active area of 0.20 cm^2.

Concentration of TBPP (M)	J_{sc} [mA cm^{-2}]	V_{oc} [V]	FF	η [%]
0	5.28	0.72	0.591	2.24
0.05	5.42	0.73	0.600	2.37
0.5	6.35	0.74	0.582	2.74
1	6.38	0.82	0.580	3.03
2	5.56	0.78	0.578	2.51

3.2. Photovoltaic performance and electrical impedance analysis

During the course of our study, to optimize the concentration of TBPP additive in the electrolyte solution, five electrolytes are developed for DSSCs and are containing 0.1 M LiI, 0.05 M I_2, 0.5 M TBP, 0.6 M BDMII with different concentrations of TBPP (0, 0.05, 0.5, 1 and 2 M). The photovoltaic parameters of the DSSCs employing the TPA sensitizer, about 14 μm thin transparent nanoporous TiO_2 (P25) film, and the redox electrolytes under simulated sunlight at 100 mW cm^{-2} are compared in Table 2 and so the photocurrent density–voltage (J–V) curves are shown in Fig. 1. Interestingly, the data for all concentrations of additive in the iodide/triiodide electrolyte indicates an increase in short circuit current density and the open circuit voltage in comparison with the standard electrolyte

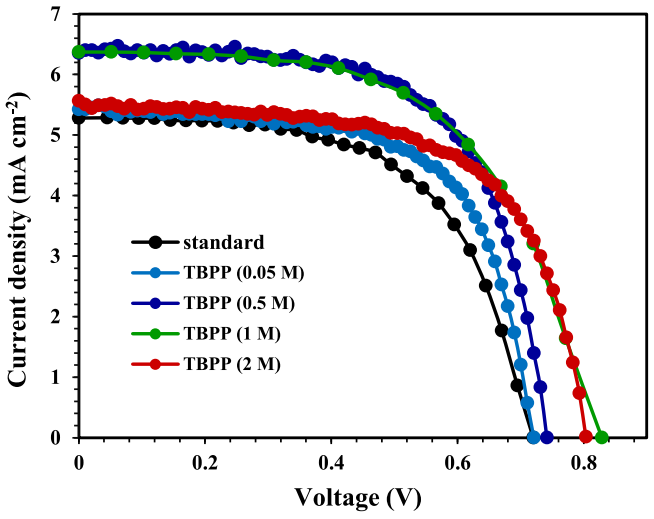

Fig. 1. J–V characteristics of DSSCs with various concentrations of TBPP in the electrolyte under 100 mW cm^{-2} illumination (AM 1.5 G).

(Fig. 2a and b), while for FF there are very small differences between all devices (Fig. 2c).

The values for the J_{sc}, V_{oc} and fill factor (FF) of the DSSCs based on electrolyte with 0.05 M of TBPP additive were 5.42 mA cm^{-2}, 0.73 V and 0.600, respectively, yielding a conversion efficiency (η) of 2.37%. Overall, among the different concentrations of TBPP additive in the redox mediators is obtained the best energy conversion efficiency of 3.03% that is achieved for 1 M of TBPP and is the highest reported for DSSCs constructed with our modified electrolyte based on TPA dye. In this concentration of additive, we observed a 14% increase in V_{oc} along with a 21% increase in J_{sc} that were explainable for the obtained efficiency increase from 2.24% (no additive) to 3.03%. This cell yielded an improvement of an additional 35% in efficiency (3.03%). However, the electrolyte containing 2 M of TBPP exhibits a decrease in efficiency (2.51% in comparison with efficiency 3.03% for cell with the electrolyte containing 1 M of TBPP). The more concentration of the additive in this device leads to decrease the concentration of the other components which causes to decrease in the electron transfer because we have prepared all electrolytes in the same volume and the more concentration of the additive (2 M) leads to decrease in the concentration of the redox species (I^-/I_3^-) which causes to decrease in the electron transfer. This effect is revealed in decreasing J_{sc} value.

In this study, when we apply the TBPP as additive, an increase in both J_{sc} and V_{oc} is observed for modified electrolytes that lead to a remarkable enhancement in the power conversion efficiency. Fig. 2a shows a significant increase in cell voltages for all concentrations. Scheme 2 shows that the improvement of V_{oc} is ascribed to a shift of the E_F of TiO_2 in the presence of TBPP molecules. So, an enlarged energy difference between of the CB of TiO_2 and the redox potential electrolyte is observed. The higher J_{sc} in devices with modified electrolyte in comparison with standard electrolyte is due to the adsorption of TBPP on the TiO_2 surface that results in the suppression of electron recombination from the CB of TiO_2 to the triiodide ions in the electrolyte (Fig. 2b).

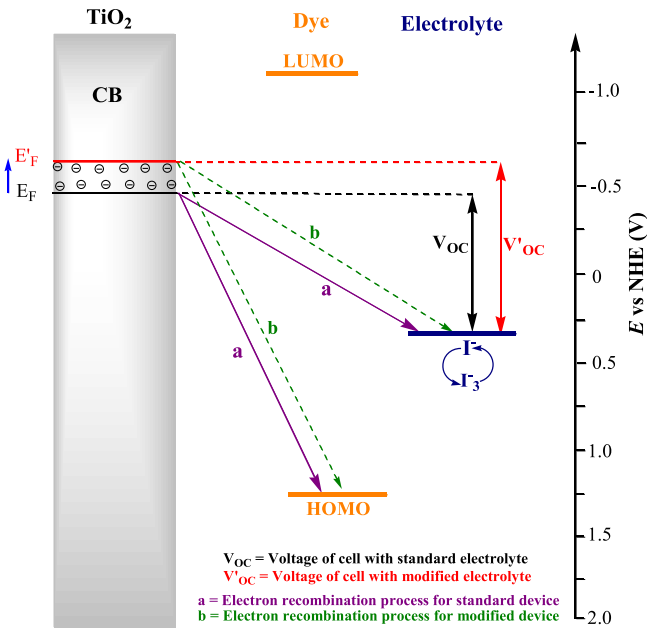

Scheme 2. Simple energy level diagram for DSSCs. The electron recombination processes are indicated by a and b arrows. The potentials for DSSCs based on the TiO_2, TPA dye and the iodide/triiodide redox couples are shown.

Two possible resonance structures for TBPP molecule have been shown in Fig. 3. The π-bond of the phosphoryl group breaks and its electron pair moves into the oxygen. This leads to the negative charge on the oxygen where it is electron donor to

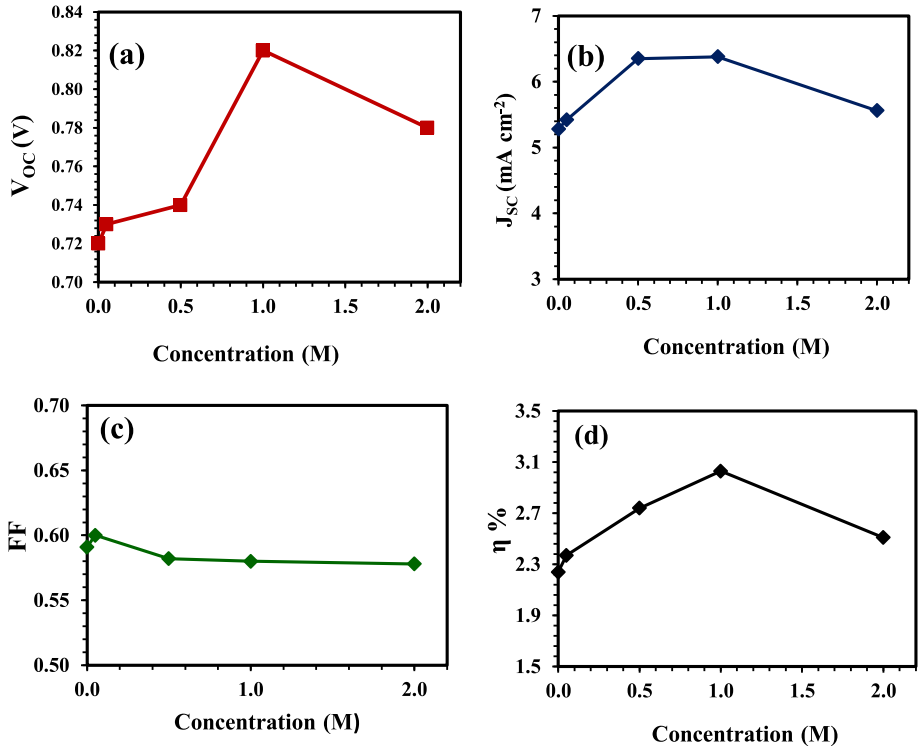

Fig. 2. Dependence of DSSC parameters on the TBPP concentration present in the electrolyte: (a) open circuit voltage (V_{oc}); (b) short circuit current (J_{sc}); (c) fill factor (FF); (d) energy conversion efficiency (η).

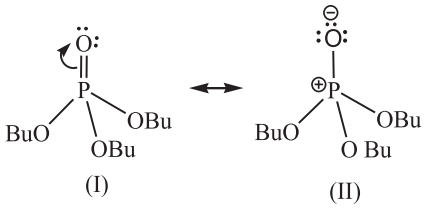

Fig. 3. Resonance structures of tributyl phosphate molecule.

TiO_2. As this π bond is broken, a positive charge places on phosphorus atom in the phosphate group (Form II). Adsorption of TBPP on the TiO_2 surface is caused interaction between the lone electron pair of oxygen in phosphate molecule and titanium (IV) which is a Lewis acid (Fig. 4) [37]. So, a shift for the E_F in the TiO_2 occurs that arises from accumulation of electrons in the CB (Scheme 2).

The influence of additives on the E_F of TiO_2 and the potential of redox couple in the electrolyte can be study by ESI and CV measurements, respectively [42–44]. To elucidate the interfacial charge transfer processes in the devices, it is necessary to investigate electrochemical properties by EIS [45–48]. Fig. 5 demonstrates typical Nyquist plots of the DSSCs with standard electrolyte and modified electrolyte with TBPP in 1 M concentration. With increasing frequency, two semicircles are observed in the Nyquist plots. The first (smaller) semicircle is attributed to the charge transfer resistance between redox ions and platinum counter electrode (R_{CE}). In the middle frequency region, second (larger) semicircle reflecting the charge transfer resistance at the dyed-TiO_2/electrolyte interface that is related to charge recombination process (R_{CT}) and can be expressed by Eq. (1) [45,49]:

$$R_{CT} = R_0 \exp\left[-\frac{\beta V}{k_B T}\right] = R_0 \exp\left[-\frac{\beta}{k_B T}(E_F - E_{redox})\right] \quad (1)$$

here, R_0 is a constant; also β is a constant that is called transfer coefficient. The k_B and T represent the Boltzmann constant and absolute temperature. E_F is the Fermi level in CB of the TiO_2 semiconductor and E_{redox} is the energy of the iodide/triiodide redox couple in the electrolyte.

To further analyze the mechanism of TBPP additive, the impedance spectra of the device with the best energy conversion efficiency and reference cell were fitted to a simplified version of the equivalent circuit (Fig. 5). The some important parameters of the working electrodes in two devices were determined from the second semicircles in Fig. 5 that the results have been summarized in Table 3. The effective diffusion coefficient of electrons (D_{eff}) can be determined by Eq. (2):

$$D_{eff} = \left[\frac{R_{CT}}{R_{CE}}\right] L^2 k_{eff} \quad (2)$$

where L is film thickness and k_{eff} is the reaction rate constant for the electron recombination with triiodide. k_{eff} is obtained by the

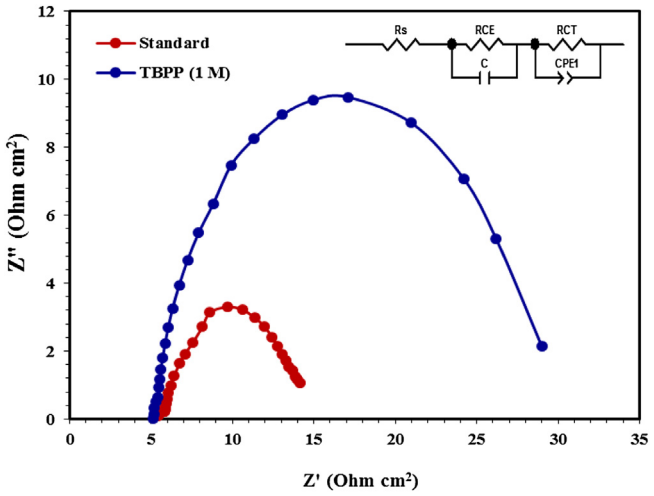

Fig. 5. Electrochemical impedance spectra for devices with standard and modified electrolytes (the inset shows equivalent circuit for EIS).

electron lifetime (τ) and angular frequency (ω_{max}) at the second (larger) semicircles in the Nyquist plots of the DSSCs (Eqs. (3) and (4)) [45]:

$$\tau = \frac{1}{\omega_{max}} \quad (3)$$

$$k_{eff} = \frac{1}{\tau} \quad (4)$$

For the R_{CE} at the counter electrode/electrolyte interface, there is small difference between two devices. This result shows that the addition of TBPP do not make the over potential at the counter electrode.

Notably, the fitted value of R_{CT} for cell with modified electrolyte is found ~27 Ω cm^2, while the corresponding value for device with standard electrolyte is ~9 Ω cm^2. This significant increase in R_{CT} shows that the addition of TBPP is more favorable to suppress the charge recombination process (b arrows in Scheme 2) that arises from electrons in TiO_2 film with triiodide in electrolyte solution and leads to increase J_{sc} [37]. On the other hand, the adsorption of TBPP on the TiO_2 surface causes to increase in electron density in CB of TiO_2. The oxygen atom in phosphoryl group acts as an electron donor when it bonded with titanium (IV) in the surface for formation of P–O–Ti bond. The combined effects of decreased charge recombination and forming the P–O–Ti bond lead to accumulation of electrons in the TiO_2. Also CPE1 is attributed to the chemical capacitances at the dyed-TiO_2/electrolyte interface [45], so, the higher CPE1 of the cell with TBPP additive arises from the accumulation of electrons (negative charge) in the TiO_2 film and the positive charge in the phosphate group (Figs. 4 and 5). In the cell based on modified electrolyte, the middle-frequency peak in the Nyquist plot shifts to lower frequency relative to standard electrolyte, exhibiting a longer electron lifetime for this electrolyte. This

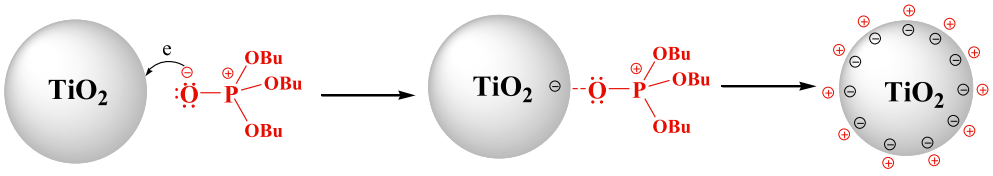

Fig. 4. Interaction between the lone electron pair of oxygen in phosphate molecule and titanium (IV) in the TiO_2.

Table 3
Electrochemical parameters obtained by fitting the impedance spectra of DSSCs with standard and modified electrolyte.

Sample	k_{eff} (s^{-1})	R_{CT} (Ω cm^2)	D_{eff} (cm^2 s^{-1})	R_{CE} (Ω cm^2)	τ (s)	n_s (cm^{-3})
Standard	10	9	2.23E-04	0.58	0.10	1.69E+19
TBPP (1 M)	2.8	26.8	1.13E-04	0.95	0.36	2.05E+19

result is in accord with the observed shift in the E_F of TiO_2 and the increase in open circuit voltage value (Scheme 2).

The cyclic voltammetry was performed to extract the potential of iodide/triiodide in the standard electrolyte and in the presence of TBPP additive in modified electrolyte (Fig. 6). The CV curves of the iodide/triiodide redox system show that adding the TBPP additive has no effect on the potential of redox couple (in region from 0.4 to 0.8 V). It indicates that TBPP additive has not any interaction with iodide and triiodide ions while the obtained results from EIS data prove existence of the interaction between the TBPP additive and TiO_2 surface (Fig. 4).

Finally, this means that TBPP additive could modify the TiO_2/electrolyte interface to reduce charge recombination from the CB of TiO_2 to the electrolyte ions and increase electron density in the CB of TiO_2, which result in the higher V_{oc} and J_{sc}, respectively, as well as the superior conversion efficiency.

4. Conclusions

To sum up, this study was performed on modified redox mediator systems in DSSCs to achieve the remarkable enhancement of cell performance. Using different concentrations of TBPP leads to a large increase of V_{oc} that has been attributed to the suppressed electron recombination in the dyed-TiO_2/electrolyte interface and in result an overall power conversion efficiency from 2.24% to 3.03%. The highest η was obtained for the DSSC based on the electrolyte for optimum concentration and electrical impedance analysis revealed a large R_{CT} for this device that showed a decrease in charge recombination. Also, surface treatment of TBPP molecules with TPA-sensitized titania films improved J_{sc} that rose of electron donor property of phosphoryl group in TBPP and accumulation of electrons in the CB of TiO_2. This discovery shed light on the future for designing simplified electrolyte systems using a variety of additives with different electron donor groups and have us a new perspective to enhance the efficiency for DSSCs by introducing a novel molecular adsorption mode on the semiconductors.

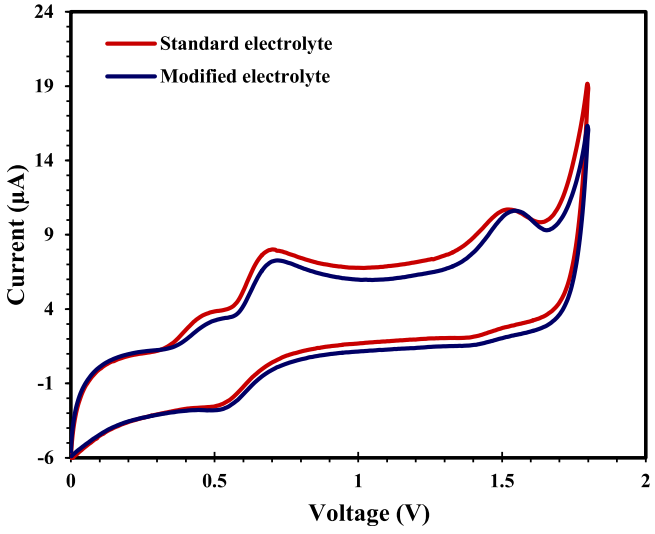

Fig. 6. Cyclic voltammograms for the standard electrolyte and modified electrolyte with TBPP in the concentration of 1 M.

Acknowledgments

The authors gratefully acknowledge from the University of Kashan for supporting this project by Grant No. 159183/17.

References

[1] M. Gratzel, Acc. Chem. Res. 42 (2009) 1788–1798.
[2] Z.S. Wang, H. Kawauchi, T. Kashima, H. Arakawa, Coord. Chem. Rev. 248 (2004) 1381–1389.
[3] A. Hagfeldt, G. Boschloo, L. Sun, L. Kloo, H. Pettersson, Chem. Rev. 110 (2010) 6595–6663.
[4] B. O'Regan, M. Gratzel, Nature 353 (1991) 737–740.
[5] J. Burschka, N. Pellet, S.J. Moon, R. Humphry-Baker, P. Gao, M.K. Nazeeruddin, M. Gratzel, Nature 449 (2013) 316–319.
[6] J.R. Jennings, Y. Liu, Q. Wang, S.M. Zakeeruddin, M. Gratzel, Phys. Chem. Chem. Phys. 13 (2011) 6637–6648.
[7] Z. Yu, N. Vlachopoulos, M. Gorlov, L. Kloo, Dalton Trans. 40 (2011) 10289–10303.
[8] S. Nakade, T. Kanzaki, W. Kubo, T. Kitamura, Y. Wada, S. Yanagida, J. Phys. Chem. B 109 (2005) 3480–3487.
[9] O. Schwarz, D. Loyen, S. Jockusch, N.J. Turro, H. Durr, J. Photochem. Photobiol. A 132 (2000) 91–98.
[10] H.J. Snaith, L. Schmidt-Mende, Adv. Mater. 19 (2007) 3187–3200.
[11] B. O'Regan, L. Xiaoe, T. Ghaddar, Energy Environ. Sci. 5 (2012) 7203–7215.
[12] T. Maeda, S. Mineta, H. Fujiwara, H. Nakao, S. Yagi, H. Nakazumi, J. Mater. Chem. A 1 (2013) 1303–1309.
[13] H. Tanaka, A. Takeichi, K. Higuchi, T. Motohiro, M. Takata, N. Hirota, J. Nakajima, T. Toyoda, Sol. Energy Mater. Sol. Cells 93 (2009) 1143–1148.
[14] C. Zafer, B. Gultekin, C. Ozsoy, C. Tozlu, B. Aydin, S. Icli, Sol. Energy Mater. Sol. Cells 94 (2010) 655–661.
[15] T. Kitamura, M. Ikeda, K. Shigaki, T. Inoue, N.A. Anderson, X. Ai, T. Lian, S. Yanagida, Chem. Mater. 16 (2004) 1806–1812.
[16] Md. Akhtaruzzaman, A. Islam, F. Yang, N. Asao, E. Kwon, S.P. Singh, L. Han, Y. Yamamoto, Chem. Commun. 47 (2011) 12400–12402.
[17] R. Chen, X. Yang, H. Tian, L. Sun, J. Photochem. Photobiol. A 189 (2007) 295–300.
[18] S.E. Koops, P.R.F. Barnes, B. O'Regan, J.R. Durrant, J. Phys. Chem. C 114 (2010) 8054–8061.
[19] K.R.J. Thomas, J.T. Lin, Y.C. Hsu, K.C. Ho, Chem. Commun. (2005) 4098–4100.
[20] P. Peumans, S.R. Forrest, Appl. Phys. Lett. 79 (2001) 126–128.
[21] M.G. Walter, A.B. Rudine, C.C. Wamser, J. Porph. Phthal. 14 (2010) 759–792.
[22] C.L. Wang, C.M. Lan, S.H. Hong, Y.F. Wang, T.Y. Pan, C.W. Chang, H.H. Kuo, M.Y. Kuo, E.W.G. Diau, C.Y. Lin, Energy Environ. Sci. 5 (2012) 6933–6940.
[23] A. Yella, H.W. Lee, H.N. Tsao, C. Yi, A.K. Chandiran, M.K. Nazeeruddin, E.W.G. Diau, C.Y. Yeh, S.M. Zakeeruddin, M. Gratzel, Science 334 (2011) 629–634.
[24] M. Mojiri-Foroushani, H. Dehghani, N. Salehi-Vanani, Electrochim. Acta 92 (2013) 315–322.
[25] W.M. Campbell, K.W. Jolley, P. Wagner, K. Wagner, P.J. Walsh, K.C. Gordon, L. Schmidt-Mende, M.K. Nazeeruddin, Q. Wang, M. Gratzel, D.L. Officer, J. Phys. Chem. C 111 (2007) 11760–11762.
[26] S. Erten-Ela, M. Marszalek, S. Tekoglu, M. Can, S. Icli, Curr. Appl. Phys. 10 (2010) 749–756.
[27] W. Wu, J. Yang, J. Hua, J. Tang, L. Zhang, Y. Long, H. Tian, J. Mater. Chem. 20 (2010) 1772–1779.
[28] L. Zhou, C. Jia, Z. Wan, X. Chen, X. Yao, Org. Electron. 14 (2013) 1755–1762.
[29] J.Y. Su, C.H. Tsai, S.A. Wang, T.W. Huang, C.C. Wu, K.T. Wong, RSC Adv. 2 (2012) 3722–3728.
[30] A. Abbotto, N. Manfredi, C. Marinzi, F.D. Angelis, E. Mosconi, J.H. Yum, Z. Xianxi, M.K. Nazeeruddin, M. Gratzel, Energy Environ. Sci. 2 (2009) 1094–1101.
[31] J. Shi, B. Peng, J. Pei, S. Peng, J. Chen, J. Power Sources 193 (2009) 878–884.
[32] M.K. Nazeeruddin, A. Kay, I. Rodicio, R. Humphry-Baker, E. Mueller, P. Liska, N. Vlachopoulos, M. Gratzel, J. Am. Chem. Soc. 115 (1993) 6382–6390.
[33] H. Kusama, H. Arakawa, H. Sugihara, J. Photochem. Photobiol. A 171 (2005) 197–204.
[34] H. Kusama, Y. Konishi, H. Sugihara, H. Arakawa, Sol. Energy Mater. Sol. Cells 80 (2003) 167–179.
[35] J.E. Benedetti, M.A. Paoli, A.F. Nogueira, Chem. Commun. (2008) 1121–1123.
[36] M. Gratzel, J. Photochem. Photobiol. A 164 (2004) 3–14.
[37] M. Cai, X. Pan, W. Liu, J. Sheng, X. Fang, C. Zhang, Z. Huo, H. Tian, S. Xiao, S. Dai, J. Mater. Chem. A 1 (2013) 4885–4892.
[38] W. Xu, B. Peng, J. Chen, M. Liang, F. Cai, J. Phys. Chem. C 112 (2008) 874–880.

[39] Q. Wang, W.M. Campbell, E.E. Bonfantani, K.W. Jolley, D.L. Officer, P.J. Walsh, K. Gordon, R. Humphry-Baker, M.K. Nazeeruddin, M. Gratzel, J. Phys. Chem. B 109 (2005) 15397–15409.
[40] L.Y. Lin, C.H. Tsai, K.T. Wong, T.W. Huang, C.C. Wu, S.H. Chou, F. Lin, S.H. Chen, A.I. Tsai, J. Mater. Chem. 21 (2011) 5950–5958.
[41] C. Teng, X. Yang, S. Li, M. Cheng, A. Hagfeldt, L. Wu, L. Sun, Chem. Eur. J. 16 (2010) 13127–13138.
[42] X. Yin, W. Tan, J. Zhang, Y. Weng, X. Xiao, X. Zhou, X. Li, Y. Lin, Colloids Surf. A 326 (2008) 42–47.
[43] V. Suryanarayanan, K. Lee, J. Chen, K. Ho, J. Electroanal. Chem. 633 (2009) 146–152.
[44] Y. Qiu, S. Lu, S. Wang, X. Zhang, S. He, T. He, J. Power Sources 253 (2014) 300–304.
[45] M. Adachi, M. Sakamoto, J. Jiu, Y. Ogata, S. Isoda, J. Phys. Chem. B 110 (2006) 13872–13880.
[46] T. Hoshikawa, T. Ikebe, R. Kikuchi, K. Eguchi, Electrochim. Acta 51 (2006) 5286–5294.
[47] J. Bisquert, J. Phys. Chem. B 106 (2002) 325–333.
[48] T. Hoshikawa, R. Kikuchi, K. Eguchi, J. Electroanal. Chem. 588 (2006) 59–67.
[49] Q. Wang, S. Ito, M. Gratzel, F. Fabregat-Santiago, I. Mora-Sero, J. Bisquert, T. Bessho, H. Imai, J. Phys. Chem. B 110 (2006) 25210–25221.